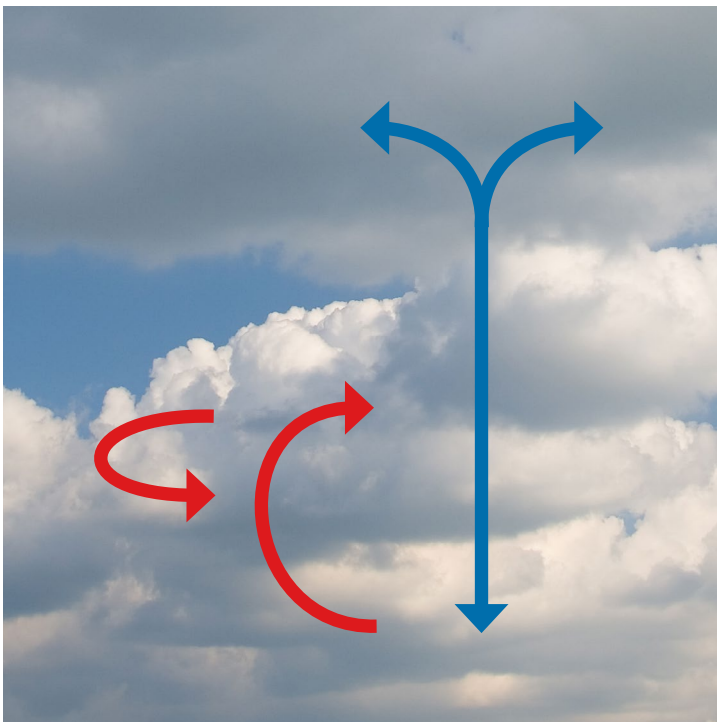


ECMWF Feature article

from Newsletter Number 164 – Summer 2020

METEOROLOGY

IFS upgrade greatly improves
forecasts in the stratosphere



Cover Photo: mm88 / iStock / Getty Images Plus

www.ecmwf.int/en/about/media-centre/media-resources

doi: 10.21957/b72xo6ms93

This article appeared in the *Meteorology* section of *ECMWF Newsletter No. 164 – Summer 2020*, pp. 18–23.

IFS upgrade greatly improves forecasts in the stratosphere

Michael Sleigh, Philip Browne, Chris Burrows, Martin Leutbecher,
Thomas Haiden, David Richardson

On 30 June 2020, ECMWF implemented a substantial upgrade of its Integrated Forecasting System (IFS). IFS Cycle 47r1 includes changes in the forecast model and in the data assimilation system. The upgrade has had a small positive impact on forecast skill in medium-range and extended-range forecasts in the troposphere and a large positive impact on analyses and forecasts in the stratosphere. The latter is mainly due to reduced large-scale biases.

Cycle 47r1 is the culmination of work from many ECMWF staff and it brings several changes. The main ones are:

- in data assimilation: revised model error in weak-constraint 4D-Var data assimilation; situation-dependent skin temperature background error variances from the Ensemble of Data Assimilations (EDA); shorter time step in the last 4D-Var minimisation; first guess in delayed cut-off 12-hour 4D-Var obtained from 8-hour Early Delivery Data Assimilation
- in the use of observations: revised ATMS (Advanced Technology Microwave Sounder) observation errors; spline interpolation introduced in the 2D GPS-RO (radio occultation) bending angle operator
- in the forecast model: quintic vertical interpolation in semi-Lagrangian advection; modified Charnock parameter for high wind speeds in tropical cyclones; 6-component MODIS (Moderate Resolution Imaging Spectroradiometer) albedo over land.

Data assimilation

In Cycle 47r1, the covariances controlling the model bias estimate in weak-constraint 4D-Var have been revised. The previous weak-constraint 4D-Var corrected only a small fraction of the model bias above 40 hPa, while the revised weak-constraint implementation better corrects the diagnosed cold and warm biases of the model above 100 hPa, reducing the mean error by up to 50%. Results show that biases in the upper stratosphere between 11 hPa and 1.5 hPa are also significantly reduced in the new system. For more details, see Laloyaux & Bonavita (2020).

Another important contribution to Cycle 47r1 is a change in the estimate of the background error variance for skin temperature over land, from constant values to spatially varying, situation-dependent variances derived from the EDA. This affects the assimilation of microwave and infrared (IR) radiance observations of the mid- and lower troposphere, which typically contain a contribution of radiation emitted from the surface. The EDA estimate was activated over land surfaces initially, where the magnitude of skin temperature errors can be very heterogeneous in space and time.

The time step in the last 4D-Var minimisation has been reduced in this new cycle from 900 seconds to 450 seconds. With this change, the inner loop and outer loop time steps match. This avoids different gravity wave speeds between the tangent-linear model (used in the computation of the final increment as part of the last inner loop) and the nonlinear model (outer loop). In the semi-implicit advection scheme of the IFS, the gravity wave speed depends on the time step. The change brings multiple benefits: clear improvements to stratospheric analyses and forecasts, and a smaller but statistically significant impact on tropospheric skill; monotonic convergence of incremental 4D-Var in some atmospheric situations, such as sudden stratospheric warming events; and an improved initial balance of the 4D-Var analysis.

The concept of continuous data assimilation introduced in Cycle 46r1 has been extended by using the analyses from each 8-hour Early Delivery Data Assimilation (DA) window as first guesses for the 12-hour Long-Window Data Assimilation (LWDA). From Cycle 47r1, the LWDA analysis can be viewed as a time extension of the DA analysis. There is no change in the background state for the LWDA, but the first minimisation is provided with a more accurate starting point. For more details, see Hólm et al. (2020).

As a result of this change, the analysis increments in LWDA increase, mainly due to the fact that more information is extracted from observations. This leads to an apparent degradation of forecasts when they are verified against own analyses. In reality, forecasts have not deteriorated but the analysis against

which they are assessed has changed. When verified against an independent analysis, like reanalysis, the impact on forecast skill from this change is neutral overall. An important benefit of this change is that it allows 4D-Var to more effectively initialise non-linear processes. Short-range forecasts are closer to observations in particular for observations which are more non-linearly related to the model state, such as radiances sensitive to water vapour, cloud and precipitation.

Use of observations

The use of hyperspectral IR data (AIRS, IASI, CrIS instruments) has been enhanced in Cycle 47r1 by allowing high-peaking channel radiances to be assimilated in locations where lower-peaking channels are rejected due to aerosol contamination. Up to Cycle 46r1, the aerosol detection scheme rejected entire IR spectra if aerosol was detected in any channel. The number of assimilated IR observations has increased by up to 5% for stratospheric channels due to this enhancement. The change is most effective in regions where aerosol (particularly Saharan dust) occurs most frequently.

In Cycle 47r1, a consistent formulation of the inter-channel error correlations was introduced for ATMS from the Suomi-NPP and NOAA-20 satellites. This change results in small but consistent improvements to first-guess fits to independent observations such as AMSU-A and the IR humidity sounding channels, indicating improved short-range forecasts of tropospheric temperature and humidity.

From Cycle 47r1, a bilinear interpolation replaces the nearest-neighbour interpolation in the computation of forecast departures for all-sky microwave radiance observations for most variables. These include temperature and humidity but not cloud hydrometeors and not the land–sea mask, for which nearest-neighbour interpolation is preferable. This change results in significantly improved first-guess fits to all-sky microwave imager and sounder radiances.

In Cycle 47r1, an improved interpolation approach has been introduced in the GPS-RO observation operator for bending angles. This revision of the interpolation ensures that refractivity gradients are continuous in the vertical and produce more realistic profiles of bending angle variability. The change leads to a small increase in the standard deviation of GPS-RO first guess departures due to the intended increase in variability, but the analysis departures are slightly improved.

Forecast model

In Cycle 47r1, the advection of temperature and humidity has been changed by increasing the order of the vertical interpolation in the semi-Lagrangian scheme from three to five. This quintic interpolation in the semi-Lagrangian advection alleviates an unphysical cooling of the IFS model in the stratosphere at high horizontal resolution. The change and its impact are described in detail in Polichtchouk et al. (2020).

A number of improvements have been made to the specification of the shortwave albedo of the land surface, snow and sea ice. The land-surface albedo is based on a monthly climatology derived from the MODIS instrument. Until Cycle 46r1, it consisted of separate albedos for direct and diffuse solar radiation in two spectral regions: ultraviolet/visible, and near-IR. Albedo for direct solar radiation was computed assuming an overhead sun, for which albedo is systematically lower than for other sun angles. In Cycle 47r1, the dependence of the direct albedo on solar zenith angle is represented following Schaaf et al. (2002). This requires six climatological fields, three in each of the two spectral regions. This tends to increase the albedo of snow-free land surfaces, on average. In addition, the albedo for the 0.625–0.778 μm band of the shortwave radiation scheme has been determined by a weighted average of the MODIS albedos for the ultraviolet/visible and the near-IR, instead of using the latter only. The improved albedo for this spectral band justified the removal of an artificial adjustment of the limits of the prognostic snow albedo, and the introduction of spectrally varying snow albedos consistent with MODIS observations as reported by Moody et al. (2007). These changes warm summer land areas in the model by around 0.1°C and by up to 0.3°C over North Africa, primarily due to the darkening of the land surface from the recomputed albedo in the 0.625–0.778 μm band. There is a small reduction in the root-mean-square error of temperature forecasts, which stems from a reduction in the model's cold bias in 2-metre temperature in many regions. A clear improvement in daytime temperature forecasts over the Sahara has been observed.

Two additional changes were made in the treatment of radiation: (i) the time series of total solar irradiance has been updated using data from Matthes et al. (2017), which include the 11-year solar cycle and are consistent with the latest solar measurements; (ii) the time series of concentrations of greenhouse gases have been updated (CMIP6's SSP3-7.0 / option 2). There is no detectable impact of (i) on forecasts, while (ii) slightly warms the upper stratosphere in analyses and forecasts in present-day simulations because in Cycle 47r1 CO₂ concentrations are consistent with recent measurements and slightly lower than previously used estimates of CO₂ concentrations.

The parametrization of momentum exchange with the ocean surface has been changed in Cycle 47r1. The relationship is expressed in a wind-speed-dependent drag coefficient. A considerable reduction of the drag under very strong winds (above 33 m/s) has been introduced. This change of drag over the ocean at high wind speeds yields a substantial improvement in maximum 10-metre wind speeds in intense tropical cyclones. For more details, see the article ‘Enhancing tropical cyclone wind forecasts’ in this Newsletter.

Minor changes have been made in the convection scheme in Cycle 47r1. They involve stability corrections to the mid-level and deep convective closures and reduced bounds for parcel perturbations. Furthermore, the convective inhibition diagnostic (CIN) has been revised to use virtual potential temperature instead of equivalent potential temperature. The revised CIN is now much reduced and is closer to values expected by forecasters (Figure 1).

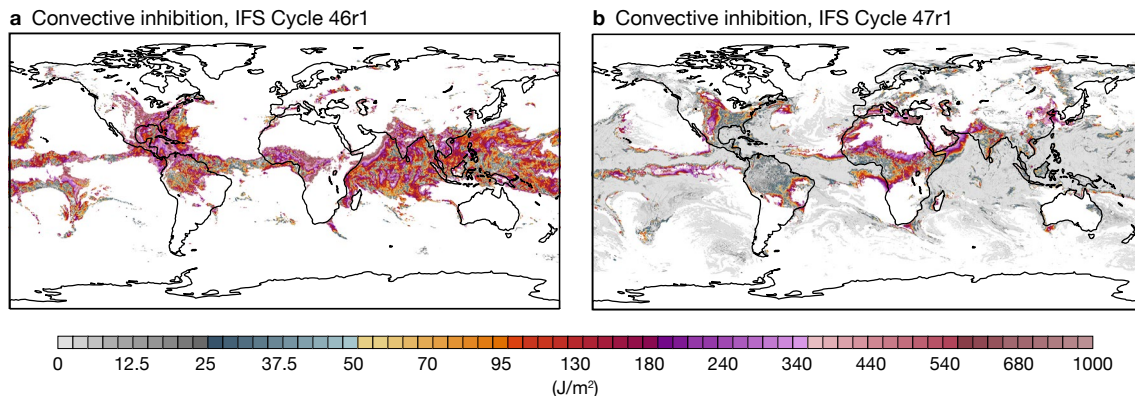


Figure 1 Three-day forecast of convective inhibition (CIN) valid at 00 UTC on 7 June 2020 for (a) IFS Cycle 46r1 and (b) IFS Cycle 47r1.

Impact on medium-range forecasts

Figures 2 and 3 show score changes and their statistical significance for the ensemble forecast (ENS) and the high-resolution forecast (HRES), respectively. HRES is run at TCo1279 resolution (corresponding to a horizontal grid spacing of about 9 km) and ENS at TCo639 (corresponding to a horizontal grid spacing of about 18 km).

The new cycle brings improvements throughout the troposphere in the order of 0.5% in extratropical forecasts. The improvements are most apparent in ENS scores, both against own analysis and against observations. In the extratropical stratosphere, the new cycle brings large improvements, such as 2–5% error reductions for temperature and geopotential at 100 hPa, and 5–15% at 50 hPa. In the tropics, there is an apparent degradation of 1–3% in upper-air scores when forecasts are verified against the new cycle’s own analyses. This does not reflect any change for the worse in the forecasts but is the result of changes to the analysis, as described above. Verification against observations shows that upper-air changes in the tropics are neutral overall, with small improvements and deteriorations balancing each other out. One exception is 250 hPa temperature in the tropics, where a deterioration of 1–3% is seen against observations. This is mainly due to a small (about +0.1 K) shift in the mean, resulting from the model changes.

The new cycle improves forecasts of several near-surface parameters, most notably 2-metre temperature and humidity (by about 0.5–1%) both in the extratropics and, when verified against observations, also in the tropics. Extratropical 10-metre wind in HRES is slightly improved, as well as total cloud cover in ENS and HRES. Tropical 10-metre wind and precipitation are slightly deteriorated. Significant wave height is mostly neutral against observations and improved against own analysis.

Impact on extended-range forecasts and model climate

The impact of Cycle 46r1 on the model climate in the extended range (up to 46 days ahead) was generally neutral. By contrast, Cycle 47r1 has a significant positive impact in the lower stratosphere, with a decrease of the cold bias in the tropics at around 50 hPa. The impact of Cycle 47r1 on weekly mean anomalies is neutral, except for some improvement in 50 hPa meridional wind, and a slight, but statistically significant, degradation in week 1 in the tropics for upper-level fields. The degradation in the fair CRPSS is consistent with a slight reduction of ensemble spread in week 1 over the tropics.

In addition to monitoring the evolution of probabilistic forecast skill scores in the scorecards, it is important to monitor the predictive skill of sources of sub-seasonal predictability, such as the Madden-Julian Oscillation (MJO). The difference in MJO bivariate correlation between Cycle 47r1 and Cycle 46r1 is not statistically significant. However, in Cycle 46r1, the MJO was too weak compared with the ERA5 reanalysis (by about 20% after day 15), and Cycle 47r1 weakens the MJO further by 3–4% in the extended range.

The seasonal forecast is not changed with Cycle 47r1. Nevertheless, the impact of the model upgrade on the model climate has been evaluated in lower-resolution seasonal forecasts. The most marked impact on the model climate in the seasonal range comes from introducing quintic vertical interpolation. This warms the equatorial and winter-hemisphere model climate stratosphere by about 0.5 K from the tropopause throughout the lower stratosphere, reducing the cold bias. Changes to the model physics have resulted in a small increase in precipitation in the Intertropical Convergence Zone (ITCZ) year-round. Longstanding biases in boreal summer zonal 10 m wind in the Indian Ocean increase slightly, worsening eastern equatorial Indian Ocean sea-surface temperature biases.

Forecast outputs

In addition to the change to convective inhibition diagnostic (CIN) described above, some other changes to the forecast outputs have been introduced with the implementation of Cycle 47r1.

The Extreme Forecast Index (EFI) for CAPE and CAPE-SHEAR now better represents 24-hour maximum values by sampling hourly values throughout the period (instead of the previous 6-hourly values).

New diagnostics of tropical cyclone (TC) size are introduced to supplement the existing forecasts of TC track and intensity (minimum central mean sea level pressure and maximum wind around a TC). TC size is represented by ‘wind radii’, which denote the furthest distance (in metres) away from the centre of the TC at which mean 10 m wind speed thresholds (34, 50 and 64 knots) are exceeded. Each of these are computed for each of four Earth-relative quadrants, i.e. NE, SE, SW and NW, delivering a total of 12 ‘size metrics’ for each TC at each time step. More details are provided by Bidlot et al. (2020) in this Newsletter.

Summary

ECMWF’s ten-year Strategy 2016–2025 describes two major avenues for further improvements in medium-range forecast skill. One is a more accurate estimation of the initial state and the consistent representation of uncertainty associated with observations and the model. The second is a better representation of model dynamics and physical processes, including interactions between different Earth system components. Cycle 47r1 includes developments in both areas. On the initial state side, it includes the revised weak-constraint 4D-Var scheme and matching time steps in the final 4D-Var outer loop, among other changes. On the modelling side, the new cycle includes quintic vertical interpolation in semi-Lagrangian advection, a modified Charnock parameter for high wind speeds occurring in tropical cyclones, and six-component MODIS albedo over land, among other changes.

The new cycle increases the forecast skill in the order of 0.5–1% in the troposphere and for some near-surface parameters, such as temperature and humidity, in the extratropics. The largest and most significant improvements from the new cycle are seen in the stratosphere, where a number of contributions have combined to address known model biases.

Further reading

Bidlot, J.-R., F. Prates, R. Ribas, A. Mueller-Quintino, M. Crepulja & Frédéric Vitart, 2020: Enhancing tropical cyclone wind forecasts, *ECMWF Newsletter* **No. 164**.

Hólm, E., S. Lang, P. Lean & M. Bonavita, 2020: Continuous long-window data assimilation, *ECMWF Newsletter* **No. 163**, 12.

Laloyaux, P. & M. Bonavita, 2020: Improving the handling of model bias in data assimilation, *ECMWF Newsletter* **No. 163**, 18–22.

Matthes, K., B. Funke, M. Anderson, L. Barnard, J. Beer, P. Charbonneau et al., 2017: Solar forcing for CMIP6 (v3. 2), *Geoscientific Model Development*, **10**, 2247–2302.

Moody, E.G., M.D. King, C.B. Schaaf, D.K. Hall & S. Platnick, 2007: Northern Hemisphere five-year average (2000–2004) spectral albedos of surfaces in the presence of snow: Statistics computed from Terra MODIS land products, *Remote Sensing of Environment*, **111**, 337–345.

Polichtchouk, I., M. Diamantakis & F. Váňa, 2020: Quintic vertical interpolation improves forecasts of the stratosphere, *ECMWF Newsletter No. 163*, 23–26.

Schaaf, C.B., F. Gao, A.H. Strahler, W. Lucht, X. Li, T. Tsang et al., 2002: First operational BRDF, albedo nadir reflectance products from MODIS. *Remote sensing of Environment*, **83**, 135–148.

© Copyright 2020

European Centre for Medium-Range Weather Forecasts, Shinfield Park, Reading, RG2 9AX, England

The content of this Newsletter is available for use under a Creative Commons Attribution-Non-Commercial-No-Derivatives-4.0-Unported Licence. See the terms at <https://creativecommons.org/licenses/by-nc-nd/4.0/>.

The information within this publication is given in good faith and considered to be true, but ECMWF accepts no liability for error or omission or for loss or damage arising from its use.